Inorg. Chem. **2005**, *44*, 4568–4575

Model for Acetylene Reduction by Nitrogenase Derived from Density Functional Theory

Johannes Kästner[†] and Peter E. Blöchl*

Institute for Theoretical Physics, Clausthal University of Technology, D-38678 Clausthal-Zellerfeld, Germany

Received January 10, 2005

The catalytic cycle of acetylene reduction at the FeMo cofactor of nitrogenase has been investigated on the basis of density functional theory. C_2H_2 binds to the same site as N_2, but it binds to a less reduced state of the cofactor. In a manner similar to that of N_2 binding, one of the sulfur bridges opens during acetylene binding. The model explains the strong noncompetitive inhibition of N_2 reduction by C_2H_2 and the weak competitive inhibition of C_2H_2 reduction by N_2. Our proposed mechanism is consistent with experimentally observed stereoselectivity and the ability of C_2H_2 to suppress H_2 production by nitrogenase.

1. Introduction

Nitrogenase, the enzyme which converts atmospheric nitrogen into ammonia,[1−6] is responsible for the supply of nitrogen to living organisms. The enzyme has two components: the Fe protein and the MoFe protein. The Fe protein is responsible for the supply of electrons. This electron transfer is driven by the hydrolysis of MgATP. The second component, the MoFe protein, contains the active site, the FeMo cofactor, which is depicted in Figure 1. The structures of both components were resolved by crystallographic analysis in 1992.[7−12] However, a central ligand of the FeMoco has been found only recently.[13] Although the central ligand could be C, N, or O according to the X-ray analysis, the consensus among theoretical studies[14−16] is that nitrogen should be assigned as the central ligand. The oxidation state of the resting state of the cofactor has been determined[15,17−19] to be $[MoFe_7S_9N]^0$ on the basis of the comparison of the theoretical results with various experimental findings.

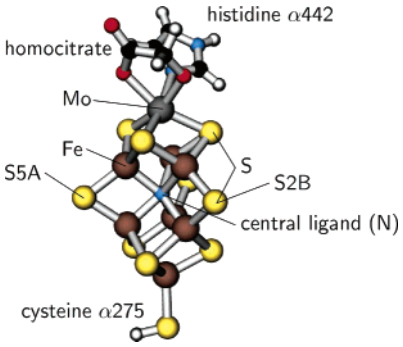

Figure 1. FeMoco with its ligands truncated as in the calculations.

Nitrogenase not only is able to catalyze the conversion of N_2 to NH_3 but also can reduce a number of other substrates.

* To whom correspondence should be addressed. E-mail: Peter.Bloechl@tu-clausthal.de.

[†] Current address: Max-Planck-Institute for Coal Research, Kaiser Wilhelm Platz 1, D-45470 Mülheim an der Ruhr, Germany.

(1) Christiansen, J.; Dean, D. R.; Seefeldt, L. C. *Annu. Rev. Plant Physiol. Plant Mol. Biol.* **2001**, *52*, 269.
(2) Burges, B. K.; Lowe, D. J. *Chem. Rev.* **1996**, *96*, 2983−3011.
(3) Smith, B. E.; Durrant, M. C.; Fairhurst, S. A.; Gormal, C. A.; Grönberg, K. L. C.; Henderson, R. A.; Ibrahim, S. K.; Le Gall, T.; Pickett, C. J. *Coord. Chem. Rev.* **1999**, *185−186*, 669.
(4) Rees, D. C.; Howard, J. B. *Curr. Opin. Chem. Biol.* **2000**, *4*, 559.
(5) Rees, D. C. *Annu. Rev. Biochem.* **2002**, *71*, 221.
(6) Igarashi, R. Y.; Seefeldt, L. C. *Crit. Rev. Biochem. Mol. Biol.* **2003**, *38*, 351.
(7) Kim, J.; Rees, D. C. *Nature* **1992**, *360*, 553.
(8) Kim, J.; Rees, D. C. *Science* **1992**, *257*, 1667.
(9) Georgiadis, M. M.; Komiya, H.; Chakrabarti, P.; Woo, D.; Kornuc, J. J.; Rees, D. C. *Science* **1992**, *257*, 1653.
(10) Chan, M. K.; Kim, J.; Rees, D. C. *Science* **1993**, *260*, 792.
(11) Peters, J. W.; Stowell, M. H. B.; Michael, S.; Soltis, S. M.; Finnegan, M. G.; Johnson, M. K.; Rees, D. C. *Biochemistry* **1997**, *36*, 1181−1187.
(12) Mayer, S. M.; Lawson, D. M.; Gormal, C. A.; Roe, S. M.; Smith, B. E. *J. Mol. Biol.* **1999**, *292*, 871.
(13) Einsle, O.; Tezcan, F. A.; Andrade, S. L. A.; Schmid, B.; Yoshida, M.; Howard, J. B.; Rees, D. C. *Science* **2002**, *297*, 1696.
(14) Hinnemann, B.; Nørskov, J. K. *J. Am. Chem. Soc.* **2003**, *125*, 1466.
(15) Lovell, T.; Liu, T.; Case, D. A.; Noodleman, L. *J. Am. Chem. Soc.* **2003**, *125*, 8377.
(16) Huniar, U.; Ahlrichs, R.; Coucouvanis, D. *J. Am. Chem. Soc.* **2004**, *126*, 2588.
(17) Schimpl, J.; Petrilli, H. M.; Blöchl, P. E. *J. Am. Chem. Soc.* **2003**, *125*, 15772.
(18) Dance, I. *Chem. Commun.* **2003**, *3*, 324.
(19) Vrajmasu, V.; Münck, E.; Bominaar, E. L. *Inorg. Chem.* **2003**, *42*, 5974.

10.1021/ic0500311 CCC: $30.25
Published on Web 05/25/2005

Investigations of alternative substrates are important because no intermediates of the N_2 conversion have been characterized experimentally; therefore one must rely on indirect information. One of the most intensely studied alternative substrates is acetylene, C_2H_2. Acetylene is converted to ethylene by

$$C_2H_2 + 2e^- + 2H^+ \rightarrow C_2H_4$$

While N_2 is fully reduced to NH_3 by the enzyme, C_2H_2 is only reduced to C_2H_4.[20] The further reduction to ethane, C_2H_6, does not take place with the wild-type enzyme.

The use of C_2D_2 as the substrate made the study of the stereoselectivity of the reduction possible. C_2D_2 is nearly completely converted to *cis*-$C_2D_2H_2$: only about 4% of the trans product is found.[21,22]

The main reason that C_2H_2 is studied more than N_2 is the fact that acetylene binds to less reduced levels of the cofactor than N_2 does. This makes it easier to access the C_2H_2 binding mode experimentally. While dinitrogen is not able to bind to FeMoco reduced by less than three electrons,[23] EPR/ENDOR experiments[24] show that C_2H_2 even interacts with the resting state of the cofactor. Kinetic studies,[25] however, conclude that C_2H_2 is reduced only after it binds to a reduced form of the enzyme.

H_2 is a necessary byproduct of the N_2 conversion process.[26] H_2 production takes reduction equivalents from N_2 reduction. In general, H_2 is also produced during the conversion of acetylene. However, in contrast to N_2, C_2H_2 is able to completely suppress hydrogen production by the enzyme at the limit of infinite partial pressure of C_2H_2.[27]

In this work, we propose a reaction mechanism for the conversion of acetylene by nitrogenase. In contrast with previous work, we not only considered the energies of possible intermediates but also calculated all of the relevant barriers. We followed the reaction path with the lowest barriers, which results in a chemically meaningful reaction cycle. Thus, we found a mechanism that was not anticipated earlier; it involves the opening of the cage of the cofactor and intermediates in which acetylene bridges two Fe atoms.

2. Computational Details

The cofactor of nitrogenase was modeled as described in our previous work on N_2 fixation.[17] We performed DFT[28,29] calculations based on the projector augmented wave[30,31] (PAW) method. The gradient-corrected PBE[32] functional was used for exchange and correlation. The planewave-based PAW method leads to the occurrence of periodic images of the structures. The electrostatic interactions between them were explicitly subtracted[33] which results in gas-phase calculations. Wave function overlap was avoided by using a unit cell large enough to keep a distance of more than 6 Å between atoms of different periodic images. We used a plane wave cutoff of 30 Ry for the auxiliary wave functions of the PAW method. For more details, see the Supporting Information.

We considered the complete FeMo cofactor with truncated ligands as shown in Figure 1. The histidine was replaced by imidazole, the homocitrate by glycolate, and the cysteine, bound to the terminal iron atom, by an SH group.

The atomic structures were optimized using damped Car−Parrinello[34] molecular dynamics with all degrees of freedom relaxed. The convergence was tested by determining if the kinetic temperature remains below 5 K during a simulation of 0.05 ps (200 time steps). During that simulation, no friction was applied to the atomic motion, and a sufficiently low friction on the wave function dynamics was chosen to avoid a noticeable effect on the atomic motion.

The transition states were determined by applying a one-dimensional constraint on the atomic positions. In this application, bond-length, angle, and torsion constraints were used. The specific constraint was varied within 1000 MD steps to determine a first upper bound for the barrier. If this upper bound is less than 20 kJ/mol, the barrier will be easily overcome, and it has not been calculated more accurately. In case of a higher estimate, the bond length was fixed to discrete values around the transition state to maximize the energy, while all unconstrained degrees of freedom were allowed to relax to minimize the energy. Proof that this approach, when converged, exactly determines the first-order transition states is given elsewhere.[35]

The FeMoco has seven high-spin iron atoms antiferromagnetically coupled to each other. Many different spin configurations may easily lead to metastable states in conventional collinear spin-polarized calculations. Therefore, we used a noncollinear description of the spin density for our calculations. In a noncollinear description, each one-electron wave function is a two-component spinor wave function.[36−39] This method not only correctly describes the truly noncollinear spin states that occur in the reaction mechanism but also avoids the artificial barriers between different spin configurations occurring in collinear calculations. Our resulting spin distribution is therefore independent of the random starting conditions. Such dependence is a common problem of conventional (collinear) spin-polarized calculations for this system, which are easily trapped in metastable spin states. We found that the spin ordering depends on subtle changes in the atomic structure. Two different collinear spin orderings, labeled BS6 and BS7, have been observed in the C_2H_2 conversion mechanism. They are shown in Figure 2. We have chosen a naming convention consistent with that of Lovell et al.[40]

We use the notation MH_x^{y+} for the oxidation and protonation state of the FeMo cofactor. In this notation, x is the number of

(20) Dilworth, M. J. *Biochim. Biophys. Acta* **1966**, *127*, 285.
(21) Fisher, K.; Dilworth, M. J.; Kim, C.-H.; Newton, W. E. *Biochemistry* **2000**, *39*, 2970.
(22) Benton, P. M. C.; Christiansen, J.; Dean, D. R.; Seefeldt, L. C. *J. Am. Chem. Soc.* **2001**, *123*, 1822.
(23) Thorneley, R. N. F.; Lowe, D. J.; Dance, I.; Sellmann, D.; Sutter, J.; Coucouvanis, D.; Pickett, C. J. *J. Biol. Inorg. Chem.* **1996**, *1*, 575−606.
(24) McLean, P. A.; True, A.; Nelson, M. J.; Lee, H.-I.; Hoffman, B. M.; Orme-Johnson, W. H. *J. Inorg. Biochem.* **2002**, *93*, 18.
(25) Lowe, D. J.; Fisher, K.; Thorneley, R. N. *Biochem. J.* **1990**, *272*, 621.
(26) Hadfield, K. L.; Bulen, W. A. *Biochemistry* **1969**, *8*, 5103.
(27) Rivera-Ortiz, J. M.; Burris, R. H. *J. Bacteriol.* **1975**, *123*, 537.
(28) Hohenberg, P.; Kohn, W. *Phys. Rev.* **1964**, *136*, B864.
(29) Kohn, W.; Sham, L. J. *Phys. Rev.* **1965**, *140*, A1133.
(30) Blöchl, P. E. *Phys. Rev. B* **1994**, *50*, 17953.
(31) Blöchl, P. E.; Först, C. J.; Schimpl, J. *Bull. Mater. Sci.* **2003**, *26*, 33.
(32) Perdew, J. P.; Burke, K.; Ernzerhof, M. *Phys. Rev. Lett.* **1996**, *77*, 3865.
(33) Blöchl, P. E. *J. Chem. Phys.* **1986**, *103*, 7422.
(34) Car, R.; Parrinello, M. *Phys. Rev. Lett.* **1985**, *55*, 2471.
(35) Blöchl, P. E.; Togni, A. *Organometallics* **1996**, *15*, 4125.
(36) Sandratskii, L. M.; Guletskii, P. G. *J. Phys. F* **1986**, *16*, L43.
(37) Kübler, J.; Hock, K.-H.; Sticht, J.; Williams, A. R. *J. Phys. F* **1988**, *18*, 469.
(38) Oda, T.; Pasquarello, A.; Car, R. *Phys. Rev. Lett.* **1998**, *80*, 3622.
(39) Hobbs, D.; Kresse, G.; Hafner, J. *Phys. Rev. B* **2000**, *62*, 11556.
(40) Lovell, T.; Li, J.; Liu, T.; Case, D. A.; Noodleman, L. *J. Am. Chem. Soc.* **2001**, *123*, 12392.

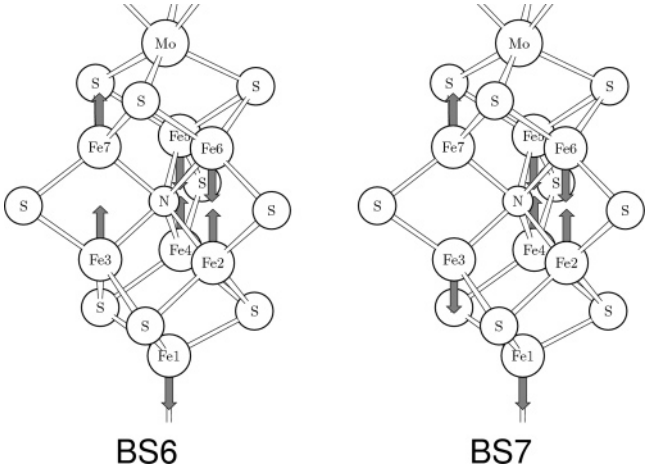

Figure 2. Two relevant spin orderings obtained for intermediates of the C_2H_2 conversion.

protons added to the unprotonated cofactor M^0, which we attribute to the resting state.[17] The total charge of the reduced and protonated cluster is given by y. Thus, $x - y$ is the number of electrons transferred to the resting state.

During the reaction, protons and electrons are transferred to the cofactor and the substrate. We made the assumption that the electron and proton transfers are coupled. This assumption implies one of two scenarios: either a reduction of the cofactor increases the proton affinity so that a proton transfer is induced or, if the proton transfer precedes the electron transfer, then the electron affinity is sufficiently enhanced by the positive charge next to the cofactor to induce an electron transfer to the cofactor. This is the main assumption in our work, besides the accuracy of the density functionals and the neglect of the protein environment, and it has been shown to be valid for the cofactor before binding of the substrate.[17]

The energies of the protons and electrons, which are consumed during the reaction, affect the overall reaction energy. It is common practice to express the energies relative to H_2 as the hydrogen source. However, the electrons and protons are not obtained from molecular hydrogen, and the reaction energies versus the energy of H_2 do not directly represent the biological system. The fact that H_2 is readily produced is a sign that H_2 is not in equilibrium with the particle reservoirs. Therefore, we define a chemical potential μ_H that reflects the biological environment. We used the formula $\mu_H = {}^1/_2E[H_2] + 35$ kJ/mol, which will be rationalized below. While the production of gaseous hydrogen, $2H^+ + 2e^- \rightarrow H_2$, is energetically neutral when using H_2 as a reference ($\mu_H = {}^1/_2E[H_2]$), as has been done in previous studies,[41−44] this reaction is exothermic by 71 kJ/mol when our μ_H is used. Additionally, we listed the reaction energies with H_2 as the reference energy in parentheses after the values we obtained with our μ_H.

Our choice of μ_H is rationalized by the following considerations. For protons, the relevant particle reservoir is the proton transfer channel, while for electrons, it is expected to be the P cluster. The exact energies cannot be determined by theory alone. As a consequence of our assumption that reduction and protonation are coupled, only the sum μ_H of the energies of the protons and electrons is relevant for the relative energies of the intermediates. A range of possible values can be derived by comparing experimental X-ray and EXAFS data with our calculated geometries: we found indirect evidence that the cofactor is unprotonated in the resting state and protonated in the reduced state.[17] Therefore, μ_H is sufficiently high to drive protonation, that is $\mu_H > E[MH] - E[M]$. On the other hand, no protonation occurs under the same conditions in the absence of MgATP. Thus the chemical potential in the absence of MgATP, denoted by μ'_H, must be sufficiently low not to drive protonation, that is, $\mu'_H < E[MH] - E[M]$. As two MgATP molecules are hydrolyzed in each electron transfer, the difference between the chemical potentials with and without MgATP is smaller than twice the energy of hydrolysis of MgATP, that is, $\mu_H - \mu'_H < 64.4$ kJ/mol.[45] It is smaller because a fraction of the energy supplied by MgATP will be dissipated. Therefore, we use the lower bound for μ_H, which is $\mu_H = E[MH] - E[M]$, in our calculations. This is the most conservative assumption possible. A less conservative value would make those reactions that include protonation more exothermic.

In this work, we evaluate not only the energetics of the intermediates but also the barriers for the transitions. This is not problematic for intramolecular rearrangements. However, to estimate the barriers for protonation, we need to simulate the proton channel. We used an ammonium molecule to mimic the proton donor. This choice affects only the barriers, not the relative energies of the intermediates.

Table 1. Energetics of the Acetylene Conversion Mechanism

state	barrier[a]	energy[b]	
M		0	(−35)
MH		0	(0)
A3	67	−11	(−11)
A1	13	−42	(−42)
A0	<25	−65	(−65)
B0	16	−186	(−151)
B1	55	−165	(−130)
$M + C_2H_4$	56	−287	(−252)

[a] The barrier refers to the reaction leading to the respective intermediate. [b] The energy is given relative to the MH state, free C_2H_2, and our choice of μ_H rationalized in Computational Details. Relative energies with H_2 as a reference are given in parentheses. All energies are given in kJ/mol.

3. Results

In this section, we will discuss the conversion of C_2H_2 to C_2H_4 step-by-step, as it emerged from our calculations. The energy profile for the reaction is shown in Figure 3. The corresponding energies and barriers are given in Table 1. The M/MH notation for the reduction and protonation states of the cofactor is described in Computational Details.

3.1. Acetylene Binding Modes. We first investigated the initial binding of acetylene to the cofactor at the MH level, which has been suggested to be the most oxidized level able to bind and reduce C_2H_2.[25] The binding modes considered in our study are shown in Figure 4.

We also considered binding to Mo. In contrast to dinitrogen, which forms at least a metastable complex with the Mo atom, C_2H_2 does not bind to Mo. This holds true even after an additional binding site was freed by cleaving one of the bonds between Mo and homocitrate. During structure relaxation, C_2H_2 spontaneously drifts away.

(41) Rod, T. H.; Hammer, B.; Nørskov, J. K. *Phys. Rev. Lett.* **1999**, *82*, 4054.
(42) Rod, T. H.; Nørskov, J. K. *J. Am. Chem. Soc.* **2000**, *122*, 12751−12763.
(43) Rod, T. H.; Logadottir, A.; Nørskov, J. K. *J. Chem. Phys.* **2000**, *112*, 5343−5347.
(44) Hinnemann, B.; Nørskov, J. K. *J. Am. Chem. Soc.* **2004**, *126*, 3920.
(45) Voet, D.; Voet, J. G.; Pratt, C. W. *Lehrbuch der Biochemie*; John Wiley & Sons: Weinheim, Germany, 2002.

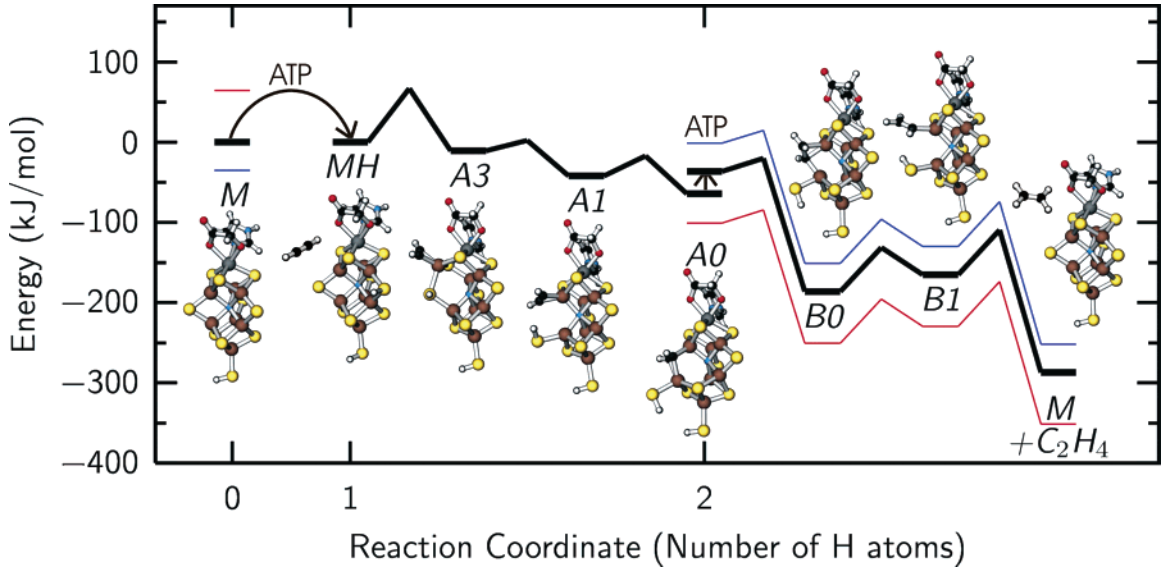

Figure 3. Energy profile of acetylene binding and reduction. Each arrow indicates a coupled reduction and protonation step. The energies for such steps depend on μ_H. The black curve is the energy profile with our choice of μ_H; the blue curve corresponds to $\mu_H = {}^1/_2E[H_2]$, and the red curve assumes that all of the energy of ATP hydrolysis is used for the reduction of the FeMoco. According to our calculations, the range between the black and the red line represents the biological reaction.

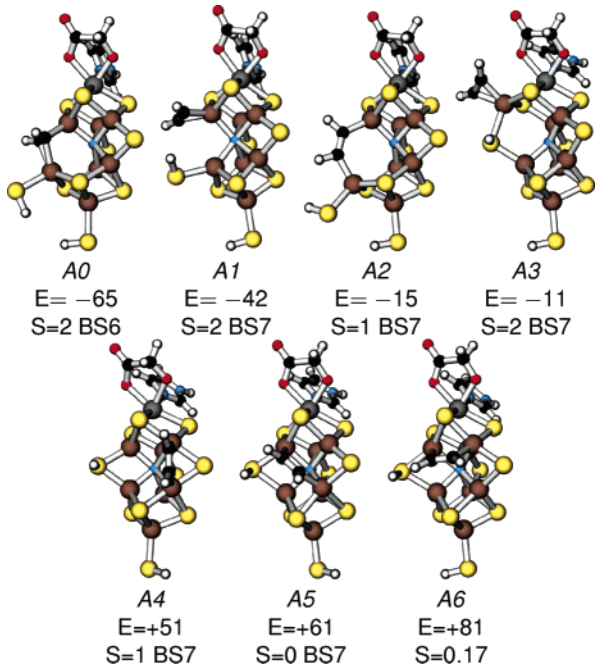

Figure 4. Binding modes of C_2H_2 at the cofactor and their binding energies at the MH level (kJ/mol) as well as their spin state. Negative energies indicate exothermic binding.

The complex of C_2H_2 with the cofactor initially forms the *A3* structure. C_2H_2 binding in *A3* is slightly exothermic with −11 kJ/mol. This complex is formed after a barrier of 67 kJ/mol, the largest barrier in the entire C_2H_2 conversion process, is overcome. This barrier is consistent with the experimental turnover rate: the rate constant for complex formation was obtained from the activation energy and an estimated attempt frequency of 3×10^{13} s^{-1} (corresponding to 1000 cm^{-1}). The rate thus obtained for C_2H_2 binding is higher than that of the association and dissociation cycle of the Fe protein and the FeMo protein.

Table 2. Geometry of Acetylene Binding Modes[a]

	A3	*A1*	*A0*	*A2*	C_2H_2	RS[b]
C−C	1.279	1.278	1.346	1.350	1.207	–
C−H	1.091	1.090	1.095	1.115	1.076	–
C−Fe3	–	3.597	2.065	1.928	–	–
C−Fe7	1.980	1.971	1.985	1.951	–	–
Fe3−Fe7	3.906	3.147	3.066	4.005	–	2.556
Fe3−N_x	1.921	2.065	3.093	3.596	–	1.968
Fe7−N_x	3.515	2.102	1.944	1.929	–	1.986
Fe3−S_μ	2.363	2.325	2.387	2.360	–	2.208
Fe7−S_μ	2.482	4.255	–	–	–	2.197
C−C−H	148.9	149.0	141.9	118.2	180.0	–
Fe−C−Fe	–	–	98.4	–	–	–

[a] Distances in Å and angles in deg. [b] Theoretical geometry of the resting state.

When C_2H_2 forms the η^2 binding mode *A3*, Fe7 loses its bond to the central ligand. Thus, the Fe atom preserves its approximate tetrahedral coordination and remains in the high-spin state. This is reminiscent of our findings for the nitrogen conversion mechanism in which the approximate tetrahedral coordination of the Fe atoms was a common structural principle.

As shown in Table 2, the C−C bond is already activated resulting in the elongation of the bond length from 1.207 Å in isolated C_2H_2 to 1.279 Å in *A3*. However, we will see below that C_2H_2 is even more strongly activated after binding to two Fe atoms.

The cofactor has an approximate 3-fold symmetry. As described earlier, we assigned the initial binding site to either Fe7 or Fe3[46] on the basis of their position next to the proton-transfer path.[17,47,48] It should be noted that, while we have chosen Fe7 as the initial binding site, Fe3 is also a likely candidate. On the basis of our work on the N_2 mechanism,[17]

(46) Our labeling of the atoms follows that of PDB entry 1M1N.
(47) Szilagyi, R. K.; Musaev, D. G.; Morokuma, K. *THEOCHEM* **2000**, *506*, 131.
(48) Durrant, M. C. *Biochem. J.* **2001**, *355*, 569.

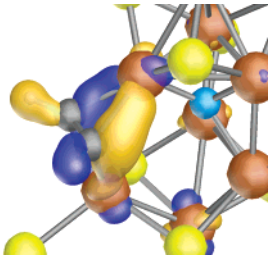

Figure 5. Activation of the C≡C triple bond through π back-donation from the iron ligands of acetylene bound in the *A0* mode. The figure illustrates an occupied minority-spin wave function with a large contribution from π back-donation.

where the two sites have been explicitly compared, we expect the two sites to be equally reactive.

Previous calculations suggested that the binding mode of acetylene, proparagyl alcohol and its reduction products, is analogous to *A3*.[49−52] As we will see later, *A3* is a relevant intermediate in our calculations but not the most stable mode. The latter is reached via a series of transformations.

In *A3*, the sulfur bridge is labilized. Its cleavage, which has a barrier of only 13 kJ/mol, leads to *A1*. With an energy of −42 kJ/mol relative to isolated C_2H_2, *A1* is substantially more stable than *A3*. The C−C bond length in *A1* is comparable to that of *A3*. The approximate tetrahedral coordination of the Fe atom, which loses its coordination to sulfur, is preserved by re-establishing the bond to the central ligand. The cleavage of the sulfur bridge is reminiscent of the nitrogen fixation mechanism.[17] For N_2, binding of the substrate and cleavage of the sulfur bridge occur in a concerted mechanism. For C_2H_2, however, the concerted mechanism from the separated molecules to *A1* requires the system to overcome a barrier of 76 kJ/mol. This barrier is larger than that of the two-step process, for which the largest barrier is 67 kJ/mol corresponding to the initial binding leading to *A3*. Thus, we conclude that first C_2H_2 associates, and then the sulfur bridge opens.

The intercalation of C_2H_2 between the two Fe atoms leading to *A0* proceeds readily and requires a barrier of less than 25 kJ/mol to be overcome. *A0* is, with a binding energy of 66 kJ/mol, the most stable binding mode of C_2H_2 at the cofactor encountered in our investigation. During the intercalation, a bond to the central ligand is broken to maintain the approximate tetrahedral symmetry of the Fe atom, which now forms the second bond to C_2H_2. While this preserves the high-spin state of that Fe atom, its spin direction is reversed. Thus, the spin ordering changes from BS7 in *A3* to BS6 in *A0*. A one-particle state of *A0* showing the activation of the C−C bond through π back-donation is depicted in Figure 5.

In *A0*, C_2H_2 forms a π complex with both Fe atoms. Thus, in contrast to N_2,[17] it binds with its C−C bond perpendicular to the direction of the Fe−Fe alignment. One might have expected to bridge the two iron atoms with each carbon connected to one iron atom as in *A2*, shown in Figure 4. This type of binding mode has also been suggested on the basis of the stereospecificity of the acetylene reduction.[22] The μ_2 binding mode *A2* is also analogous to the corresponding binding mode of the doubly protonated dinitrogen from the N_2 conversion. However, for C_2H_2, *A2* is 50 kJ/mol above the ground state, *A0*. Therefore, the rotation of C_2H_2 into *A2* is unfavorable.

In *A2*, the sp hybridization of isolated C_2H_2 is converted into an sp^2 hybridization. The C−C−H angles are 118.2°, even lower than the value of 121.7° for isolated C_2H_4. Two sp^2 hybrid orbitals form the bonds to the iron atoms. The C−C bond is significantly lengthened from 1.207 Å in the gas phase to 1.350 Å.

We also investigated the *A4*, *A5*, and *A6* binding modes. However, as shown in Figure 4, their energies are significantly higher than those of the other modes discussed above. Therefore, we concluded that they are not relevant for the C_2H_2 conversion process.

Structural data for the low-energy acetylene binding modes are summarized in Table 2. Fe7 represents the iron atom next to Mo, and Fe3 is located next to the terminal iron atom. Note that the larger distances, which do not correspond to chemical bonds, may depend strongly on the protein environment and thus may contain larger errors.

Table 3. C_2H_2 Binding Energies at Different Reduction and Protonation Levels[a]

	A0	*A1*	*A2*	*A3*
M	+15			+9
MH	−65	−42	−15	−11
MH_2	−87	−58	−37	

[a] Energies in kJ/mol. Negative values indicate exothermic binding. Note that these values are independent of μ_H.

3.2. Acetylene Binding Energies at Different Reduction States of the Cofactor. We have determined if binding is possible in other reduction states of the cofactor. We find that the affinity of the cofactor for C_2H_2 increases with its reduction level, as seen in Table 3. With the exception of the resting state, the energetic order of the different binding modes, however, is preserved during reduction and protonation of the cluster. While binding is significantly more stable in the MH_2 state than in the MH state, discussed above, binding is slightly endothermic in the resting state, M. We attribute the destabilization of *A0* in the resting state to the absence of the proton on the sulfur bridge, which facilitates the cleavage of the sulfur bridge. Thus *A3*, which has an intact sulfur bridge, is the most stable binding mode in the resting state.

In agreement with the experiment, our calculations predicted the reduction level MH to be the first reduction level that is able to bind C_2H_2 exothermically.

3.3. Protonation. In *A0*, acetylene is already activated, which can be seen from the bending of the H−C−C−H unit in Figure 4 and from the increase of the C−C bond length from 1.207 Å in the gas phase to 1.346 Å.

The acetylene molecule in *A0* exhibits two sp^2 hybrid orbitals as frontier orbitals. They do not point away from

(49) Dance, I. *J. Am. Chem. Soc.* **2004**, *126*, 11852.
(50) Durrant, M. C. *Biochemistry* **2004**, *43*, 6030.
(51) Igarashi, R. Y.; Dos Santos, P. C.; Niehaus, W. G.; Dance, I. G.; Dean, D. R.; Seefeldt, L. C. *J. Biol. Chem.* **2004**, *279*, 34770.
(52) Lee, H.-I.; Igarashi, R. Y.; Laryukhin, M.; Doan, P. E.; Dos Santos, P. C.; Dean, D. R.; Seefeldt, L. C.; Hoffman, B. M. *J. Am. Chem. Soc.* **2004**, *126*, 9563.

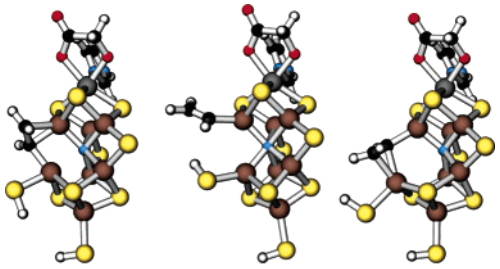

Figure 6. Intermediates after protonation of C_2H_2 at the MH reduction and protonation state. Energies are given in kJ/mol relative to dissociated C_2H_4 and M. These energies are independent of μ_H. See Figure 4 for further information.

the cluster; instead, they point in the direction of the faces of the cofactor spanned by 4 iron atoms. After reduction, one of these frontier orbitals is protonated. Thus, the proton donor has to approach the cofactor on one of these faces.

Protonation results in the cleavage of one of the two π-complex bonds and leads to structure *B0* depicted in Figure 6. The π-complex bond to the other iron atom remains intact. With NH_4^+ as the proton source, the proton transfer is exothermic by 150 kJ/mol. The barrier is 16 kJ/mol. The barrier for protonation depends on the choice of the proton donor and is expected to be less reliable than the other energies.

Following the protonation, C_2H_3 converts into a σ ligand bound to only one iron atom, resulting in structure *B1* shown in Figure 6. To avoid a three-coordinated Fe atom, the central ligand restores its 6-fold coordination. This rearrangement is endothermic by 21 kJ/mol and has a barrier of 55 kJ/mol.

We also considered a third C_2H_3 binding mode, *B2*. It has a higher energy than those discussed previously and does not play any role in the reduction process.

C_2H_3 bound to the μ^2-bridging sulfur atom, as proposed from the calculations on a smaller model,[50] can also be ruled out. It is 26 kJ/mol less stable than *B0*. Moreover, it could only be reached indirectly as it requires a closed sulfur bridge with bound substrate. Closing of the sulfur bridge induces intramolecular proton transfer and substrate cleavage, as discussed in the following section.

3.4. C_2H_4 Production. In structure *B1*, the proximal CH group and the SH group are properly positioned for an intramolecular proton transfer. It is exothermic by 122 kJ/mol. The protonation of the C_2H_3 fragment leads to C_2H_4 which is immediately displaced by the closing of the sulfur bridge. The barrier for this concerted process is 56 kJ/mol. It releases ethylene and restores the cofactor to its resting state.

This last internal proton transfer determines the stereoselectivity of the two protonations. In *B1*, the proton that has been added to C_2H_2 is in the position cis to the C−Fe bond. This C−Fe bond is in turn replaced by a C−H bond. Hence, *cis*-$C_2D_2H_2$ is produced. An isomerization of the bound C_2H_3 fragment can be excluded because of its large barrier of 169 kJ/mol for the torsion about the C═C double bond. Therefore, *cis*-$C_2D_2H_2$ is produced during the C_2D_2 conversion.

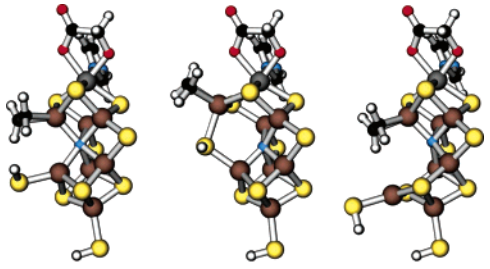

Figure 7. C_2H_4 bound to the cofactor and its binding energy in kJ/mol as well as the spin state.

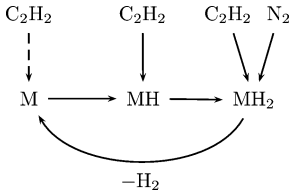

Figure 8. Scheme for the binding of C_2H_2 and N_2 to FeMoco in the wild-type MoFe protein. C_2H_2 weakly binds to the resting state M but is bound and reduced at the more reduced states MH and MH_2. In contrast, the earliest state to which N_2 binds is MH_2. Dihydrogen may be released from MH_2.

If an intermolecular protonation is assumed, C_2H_4 is not spontaneously displaced but stays weakly bound to the cofactor. Three possible binding modes and their C_2H_4 binding energies are shown in Figure 7.

4. Discussion

4.1. Inhibition. Dinitrogen was found, experimentally, to be a weak competitive inhibitor of acetylene reduction, but acetylene was found to be an effective noncompetitive inhibitor of dinitrogen reduction.[20,27,53] Our calculations support an idea proposed by Davis et al.:[54,55] acetylene binds to the cofactor at a state which is not sufficiently reduced for nitrogen to bind. Therefore, it inhibits noncompetitively because it reduces the pool of available N_2 binding sites. Dinitrogen competitively inhibits acetylene reduction at the reduced state. As most acetylene is reduced in the oxidized state, before dinitrogen can bind, the inhibition is weak.

As also illustrated in Figure 8, acetylene is able to bind and can be reduced at the MH level, while dinitrogen needs at least the more reduced MH_2 level to be effectively bound.[17] Therefore, most of the acetylene is bound and reduced at the MH level, and only a limited portion of the cofactor molecules reaches the MH_2 level. The EPR/ENDOR experiments[24] which show that acetylene already interacts with the resting state may be explained by weak and reversible binding. Our calculated binding energy of +9 kJ/mol indicates endothermic binding but does not rule out interac-

(53) Hwang, J. C.; Chen, C. H.; Burris, R. H. *Biochim. Biophys. Acta* **1973**, *292*, 256.
(54) Davis, L. C.; Wang, Y.-L. *J. Bacteriol.* **1980**, *141*, 1230.
(55) Liang, J.; Burris, R. H. *Biochemistry* **1988**, *27*, 6726.

tion. While the population of C_2H_2 bound to the resting state is small, we expect its desorption barrier to be sizable, similar to that of the MH level, which is 78 kJ/mol. Thus, C_2H_2 bound to the resting state has a sufficiently long lifetime for the observation of a characteristic EPR signal.

The statement that dinitrogen already binds at the MH_2 level should be understood in the sense that this is the reduction level of the cofactor. The MoFe protein, instead, is reduced by one additional electron in that state.[56] Thus, we expect that, under turnover conditions, the reduction level of the protein is, in general, higher by one electron than that of the cofactor. Therefore, the MH_2 reduction level for the cofactor corresponds to the E3H3 level for the protein expressed in the Thorneley−Lowe scheme.[23]

4.2. H_2 Production. Unlike N_2, C_2H_2 is able to completely suppress hydrogen production by the enzyme at the limit of infinite partial pressure of C_2H_2.[27] Previously,[17] we suggested a mechanism for H_2 formation via protonation of one Fe atom. After all of the μ^2-sulfur bridges, which are accessible to protons, are protonated, protons bind to the next most favorable binding sites, which are the Fe atoms. H_2 is produced if the hydride bound to an Fe atom recombines with the proton of the nearby sulfur bridge. Considering the proton transfer channels, only two of the three sulfur bridges are expected to be accessible to protons. Thus, H_2 production starts if a proton is transferred to the MH_2 state as shown in Figure 8. Acetylene binds to the MH state and thus suppresses the MH_2 state. Dinitrogen binding on the other hand requires the MH_2 state, which is also able to produce H_2.

4.3. Lifetime of Intermediates. Long-lived intermediates of this proposed reaction mechanism may, in principle, be observed experimentally. Therefore, it is important to know which of the intermediates has the longest lifetime. The rate-limiting step of the overall reaction is known experimentally to be the electron supply.[23] The only intermediate which depends on the rate of reduction is *A0*. Therefore, its lifetime is given by the electron-transfer rate, which is on the order of $1-10\ s^{-1}$.[56]

One of our assumptions is that protons and electrons are transferred to the cofactor in an alternating manner. If the second proton transfer precedes the reduction of the cofactor, we expect the reaction to proceed directly from *A0* to a state that is similar to *B0* but lacks one electron. We did not calculate the reaction steps following this protonation. However, if we assume that the energetics are similar to our, more reduced, model, the intermediate with the longest lifetime is *B0*. Thus, *B0* with a lifetime somewhat longer than 50 ms might be accessible for experiments.

4.4. Mutation. In the this section, we show that the present mechanism is consistent with the mutation studies performed so far.

Hisα195. The substitution of Hisα195[57] with glutamine results in an MoFe protein that hardly reduces N_2 but still reduces acetylene (and protons) at near wild-type rates,[58,59] although it produces more H_2 when reducing acetylene.[21] Hisα195 provides a hydrogen bond to the μ_2-sulfur bridge S2B and is the only proton source for that atom. This proton source is removed in the mutant strain. There are only two μ_2-sulfur bridges that can be protonated, namely, S5A and S2B. Protonation of both of them is essential for the MH_2 state to be reached without hydride formation, as discussed above. A stable MH_2 state and thus a protonated S2B is essential for N_2 reduction, while it is not essential for acetylene binding as the latter readily occurs at the MH level. H_2 production also proceeds from MH if the protonation of further sulfur bridges is not possible. In that case, a hydride is formed near S5A releasing H_2.

In Gluα195 nitrogenase, N_2 is not reduced but it still inhibits both proton and acetylene reduction. This has been interpreted by Christiansen et al.,[1] who state "that acetylene, protons, and dinitrogen must occupy the same or closely overlapping binding sites within the MoFe protein." Their interpretation is consistent with our results of possible C_2H_2 binding at the MH_2 level.

Glyα69. The substitution of Glyα69 with serine,[60] cysteine, proline, glutamate, or aspartate[1] results in an enzyme that is able to reduce N_2 at the normal rate but has a strongly suppressed rate of reduction for acetylene.[60] Furthermore, in these mutant strains, acetylene was converted from a noncompetitive inhibitor to a competitive inhibitor of dinitrogen reduction. Christiansen et al. provided a structural rationalization for these two changes on the basis of a common binding site for N_2 and C_2H_2.[1] This common binding site is confirmed by our model.

Our calculations can obviously only explain mutation studies that address residues which interact directly with the cofactor. Thus, experiments like the replacement of Glnα191 with lysine[21] lie outside of the scope of our investigations. Glnα191 is only hydrogen bound to a part of the homocitrate ligand, which is not part of our calculated model.

4.5. Multiple Binding Sites. Different EPR signals have been found during acetylene turnover in the Glnα195 mutant.[61] The interpretation was that two C_2H_2 molecules bind simultaneously to the cofactor. Using the isolated cofactor, the ligand PhSH, and a europium−amalgam cathode as reduction agent, FeMoco·PhSH has also been found to simultaneously coordinate several substrate molecules to activate them for the subsequent reactions.

We could verify that two C_2H_2 molecules can bind simultaneously to the cofactor. If one molecule is bound according to *A0*, it is possible to bind another one in an η^2 manner, as in *A1*, involving two different iron atoms. The second C_2H_2 molecule binds exothermically by 32 kJ/mol in the MH_2 level. The resulting structure is illustrated in Figure 9.

(56) Fisher, K.; Newton, W.; Lowe, D. J. *Biochemistry* **2001**, *40*, 3333.
(57) Our notation refers to the nitrogenase of *Azotobacter vinelandii*.
(58) Kim, C. H.; Newton, W. E.; Dean, D. R. *Biochemistry* **1995**, *34*, 2798.
(59) Sørlie, M.; Christiansen, J.; Lemon, B. J.; Peters, J. W.; Dean, D. R.; Hales, B. J. *Biochemistry* **2001**, *40*, 1540.
(60) Christiansen, J.; Cash, V. L.; Seefeldt, L. C.; Dean, D. R. *J. Biol. Chem.* **2000**, *275*, 11459.
(61) Sørlie, M.; Christiansen, J.; Dean, D. R.; Hales, B. J. *J. Am. Chem. Soc.* **1999**, *121*, 9457.

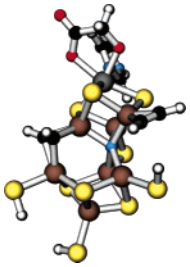

Figure 9. Two acetylene molecules simultaneously binding to the cofactor.

4.6. Stereoselectivity. While previous reports[20] showed that *Clostridium pasteurianum* produced exclusively *cis*-$C_2D_2H_2$ from C_2D_2, recent investigations[21,22] reported that small amounts (4%) of the $C_2D_2H_2$ product were the trans isomer. Production of mainly *cis*-$C_2D_2H_2$ is confirmed by our results. Production of the trans isomer would require overcoming a high barrier for a rotation around a double bond.

5. Conclusion

In contrast to N_2, the catalytic conversion of C_2H_2 to C_2H_4 by nitrogenase offers a possibility to verify a proposed mechanism by comparison with a large amount of experimental data. As C_2H_2 binds to less reduced forms of the cofactor than N_2 does, the C_2H_2 binding modes are easier to access experimentally.

We have proposed an acetylene conversion mechanism on the basis of our first-principles calculations that is in general accordance with the experimental data. It explains the noncompetitive inhibition of N_2 conversion by C_2H_2 as well as the weak competitive inhibition of C_2H_2 conversion by N_2. It also accounts for the fact that C_2H_2 can completely suppress the H_2 production of nitrogenase.

The general chemical reactivity of the cofactor with C_2H_2 is similar to its reactivity with N_2. The general common features are that a sulfur bridge is destabilized by protonation and the substrate is bound to multiple iron atoms.

The good agreement of the proposed C_2H_2 conversion supports the mechanism of N_2 conversion we found by using the same methodology.[62]

Acknowledgment. We thank HLRN for granting us access to their IBM pSeries 690 supercomputers. This work has benefited from the collaboration within the ESF program on "Electronic Structure Calculations for Elucidating the Complex Atomistic Behaviour of Solids and Surfaces".

Supporting Information Available: Computational and structural details. This material is available free of charge via the Internet at http://pubs.acs.org.

IC0500311

(62) Kästner, J.; Blöchl, P. E. *ChemPhysChem*, **2005**, in press.